Fabrication and properties of metalo-dielectric photonic crystal structures for infrared spectral region

Vygantas Mizeikis[1], Saulius Juodkazis[1], Rima Tarozaitė[2], Jurga Juodkazytė[2], Kęstutis Juodkazis[2], and Hiroaki Misawa[1*]

[1]*Research Institute for Electronic Science, Hokkaido University, N21 W10 CRIS Bldg., Sapporo 001-0021, Japan*

[2]*Institute of Chemistry, A. Goštauto 9, Vilnius LT-01108, Lithuania*

[*]*corresponding author: misawa@es.hokudai.ac.jp*

Abstract: We report structural and optical properties of three-dimensional periodic metallic woodpile structures obtained by direct laser writing in dielectric photoresist SU-8 and subsequent electroless coating by a thin Ni film. Signatures of photonic stop gaps were observed in optical reflection spectra of the structures at infrared wavelengths. This study demonstrates that the combination of DLW and chemical infiltration of metals is attractive as a simple and cost-efficient method for the fabrication of metalo-dielectric photonic crystals.

OCIS codes: (220.4000) Microstructure fabrication; (160.5470) Polymers;(350.3390) Laser materials processing;(999.999) Photonic crystals

References and links

1. M. Sigalas, C. Chan, K. Ho, and C. Soukoulis, "Metallic photonic band-gap materials," Phys. Rev. B **52**, 11744–11751 (1995).
2. D. F. Sievenpiper, M. E. Sickmiller, and E. Yablonovitch, "3D wire mesh photonic crystals," Phys. Rev. Lett. **76**, 2480–2483 (1996).
3. I. El-Kady, M. Sigalas, R. Biswas, K. Ho, and C. Soukoulis, "Metallic photonic crystals at optical wavelengths," Phys. Rev. B **62**, 15299–15302 (2000).
4. S. Enoch, J.-J. Simon, L. Escoubas, Z. Elalmy, F. L. P. Torchio, and G. Albrand, "Simple layer-by-layer photonic crystal for the control of thermal emission," Appl. Phys. Lett. **86**, 261101 (2005).
5. J. T. K. Wana and C. T. Chan, "Thermal emission by metallic photonic crystal slabs," Appl. Phys. Lett. **89**, 41915 (2006).
6. T. D. Drysdale, I. Gregory, C. Baker, E. H. Linfield, W. R.Tribe, and D. R. S. Cumming, "Transmittance of a tunable filter at terahertz frequencies," Appl. Phys. Lett. **85**, 5173 – 5175 (2004).
7. A. Ovsianikov, A. Ostendorf, and B. Chichkov, "Three-dimensional photofabrication with femtosecond lasers for applicationsin photonics and biomedicine," Appl. Surf. Sci. (2007), in press, available online, doi:10:1016/j.apsuc.2007.01.058.
8. V. Poborchii, T. Tada, T. Kanayama, and A. Moroz, "Silver-coated silicon pillar photonic crystals: enhancement of a photonic band gap," Appl. Phys. Lett. **82**, 508–510 (2002).
9. V. Mizeikis, K. K. Seet, S. Juodkazis, and H. Misawa, "Three-dimensional woodpile photonic crystal templates for infrared spectral range," Opt. Lett. **29**, 2061 – 2063 (2004).
10. K. K. Seet, V. Mizeikis, S. Matsuo, S. Juodkazis, and H. Misawa, "Three-dimensional spiral - architecture photonic crystals obtained by direct laser writing," Adv. Mat. **17**, 541 – 545 (2005).
11. M. Deubel, G. von Freymann, M. Wegener, S. Pereira, K. Busch, and C. Soukoulis, "Direct laser writing of three-dimensional photonic-crystal templates for telecommunications," Nat. Mater. **3**, 444–7 (2004).
12. K. K. Seet, V. Mizeikis, S. Juodkazis, and H. Misawa, "Spiral three-dimensional photonic crystals for telecomunications spectral range," Appl. Phys. A **82**, 683–688 (2006).
13. M. Lindblom, H. Hertz, and A. Holmberg, "SU-8 plating mold for high-aspect-ratio nickel zone plates," Microelectron. Eng. (2007), in press, available online, doi:10:1016/j.mee.2007.01.109.

#82675 - $15.00 USD Received 2 May 2007; revised 6 Jun 2007; accepted 8 Jun 2007; published 22 Jun 2007

14. F. Formanek, N. Takeyasu, T. Tanaka, K. Chiyoda, and A. I. S. Kawata, "Three-dimensional fabrication of metallic nanostructures over large areas by two-photon polymerization," Opt. Express **14**, 800 – 809 (2006).
15. V. Mizeikis, S. Juodkazis, A. Marcinkevicius, S. Matsuo, and H. Misawa, "Tailoring and characterization of photonic crystals," J. Photochem. Photobiol. C: Photochemistry Reviews **2**, 35–69 (2001).
16. V. Mizeikis, S. Matsuo, S. Juodkazis, and H. Misawa, "Femtosecond laser microfabrication of photonic crystals," in "3D laser microfabrication," , H. Misawa and S. Juodkazis, eds. (Willey-VCH Verlag, 2006), chap. 10, pp. 239–286.
17. K. K. Seet, V. Mizeikis, S. Juodkazis, and H. Misawa, "Three-dimensional circular spiral potonic crystal structures recordedby femtosecond pulses," J. Non-Crystal. Solids **352**, 2390–2394 (2006).
18. K. K. Seet, V. Mizeikis, S. Juodkazis, and H. Misawa, "Three-dimensional horizontal circular spiral photonic crystals with stopgaps below 1 μm," Appl. Phys. Lett. **88**, 221101 (2005).
19. K. M. Ho, C. T. Chan, C. M. Soukoulis, R. Biswas, and M. Sigalas, "Photonic band gaps in three dimensions: New layer-by-layer periodic structures," Solid State Commun. **89**, 413–416 (1994).
20. S. Noda, "Three-dimensional photonic crystals operating at optical wavelength region," Physica B **279**, 142–149 (2000).
21. S. Ogawa, M. Imada, S. Yoshimoto, M. Okano, and S. Noda, "Control of light emission by 3D photonic crystals." Science **305**, 227–9 (2004).
22. J. Fleming, S. Lin, I. El-Kady, R. Biswas, and K. Ho, "All-metallic three-dimensional photonic crystals with a large infrared bandgap." Nature **417**, 52–5 (2002).
23. R. Tarozaitė and A. Selskis, "Electroless nickel plating with Cu^{2+} and dicarboxylic acids additives," Trans. IMF **84**, 105 –112 (2006).
24. H. Ong, X. Yuan, S. Tao, and S. C. Tjin, "Photothermally enabled lithography for refractive-index modulation in SU-8 photoresist," Opt. Lett. **31**, 1367 – 1369 (2006).
25. T. A. Anhoj, A. M. Jorgensen, D. A. Zauner, and J. Hubner, "The effect of soft bake temperature on the polymerization of SU-8 photoresist," J. Micromech. Microeng. **16**, 1819–1824 (2006).
26. M. Ordal, L. Long, J. Bell, S. Bell, R. Alexander, and C. Ward, "Optical properties of the metals Al, Co, Cu, Au, Fe, Pb, Ni, Pd, Pt, Ag, Ti, and W in the infrared and far infrared," Appl. Opt. **22**, 1099–1120 (1983).
27. Y. V. Miklyaev, D. C. Meisel, A. Blanco, G. von Freymann, K. Busch, W. Koch, C. Enkrich, M. Deubel, and M. Wegener, "Three-dimensional face-centered-cubic photonic crystal templates by laser holography: fabrication, optical characterization, and band-structure calculations," Appl. Phys. Lett. **82**, 1284 (2003).
28. T. Kondo, S. Juodkazis, V. Mizeikis, S. Matsuo, and H. Misawa, "Fabrication of three-dimensional periodic microstructures in photoresist su-8 by phase-controlled holographic lithography," New J. Phys. **8**, 250 (2006).
29. R. Tarozaitė, M. Kurtinaitienė, A. Džiūvė, and Z. Jusys, "Composition, microstructure and magnetic properties of electroless-plated thin Co-P films," Surf. Coat. Technol. **115**, 57–65 (1999).
30. A. M. Luneckas, R. K. Tarozaitė, and I. K. Genutienė, "Properties of palladium coatings deposited using hypophosphite," Protection of metals (in Russian) **4**, 496 – 498 (1971).
31. M. Šalkauskas and A. Vaškelis, *Chemical Metallizing of Plastics*, (in Russian), (Khimiya, Leningrad, 1985).
32. A. Vaškelis, J. Jačiauskienė, A. Jagminienė, and E.Norkus, "Obtaining of 1B group metal films by novel electroless deposition method," Sol. State Sciences **4**, 1299 – 1304 (2002).

1. Introduction

Among the materials exhibiting photonic band gap (PBG) functionality, metalo-dielectric photonic crystals (MDPC) attract significant interest [1, 2, 3]. In MDPCs, discontinuities of the dielectric function at the metal-dielectric interface are much stronger than in all-dielectric photonic crystals (DPC), and consequently, significant PBG attenuation can be attained in smaller structures comprising fewer lattice periods. At infrared (IR) wavelengths, where noble metals like Au or Ar are nearly lossless, MDPCs are attractive as spectral edge-cut and band-pass filters [4, 5] whose parameters are tunable by the design of the periodic structure. Three-dimensional (3D) MDPCs can be used as filters in THz spectroscopy [6] or heat shields for low-temperature IR detectors. MDPCs with short lattice periods, though more difficult to fabricate, may operate at wavelengths close to optical and plasma regions as plasmonic crystals and left-handed (negative refractive-index) materials. MDPCs and other metallic micro- and nano-structures are widely expected to be useful in plasmonic, sensor and bio-medical applications [7].

Practical fabrication of MDPC structures is impeded by various difficulties. Extended, well-ordered periodic micro-structures with intentional defects are difficult to build even using the

#82675 - $15.00 USD Received 2 May 2007; revised 6 Jun 2007; accepted 8 Jun 2007; published 22 Jun 2007

most advanced semiconductor micro- and nano-fabrication techniques. Moreover, these techniques are not directly applicable to metals. Therefore, 3D as well as simpler two-dimensional (2D) MDPC structures are often obtained by incorporating metals into pre-fabricated dielectric templates [8]. Previously we have reported fabrication of various 3D DPC structures in commercial photoresist SU-8 using direct laser writing (DLW) technique [9, 10]. This technique allows high flexibility in the fabrication of periodic and non-periodic 3D structures, including woodpile and square/circular spiral structures [9, 10, 11, 12]. Therefore, the idea to create MDPC structures by incorporation of metals to laser-fabricated SU-8 templates seems promising.

There are different metallization techniques available, such as sputtering, evaporation, chemical vapor deposition, chemical, and electrochemical coating. All of them are capable of controllable deposition on dielectric templates of metal films thicker than optical skin-depth (typically tens of nanometers). Dielectric template coated by a metallic film of substantial thickness would become optically indistinguishable from metallic template. Chemical and electrochemical coating techniques are especially interesting, since they do not require high temperatures or low-pressure/vacuum environment, and can effectively coat inner surfaces of porous templates. Recently, fabrication of diffractive elements for soft X-ray optics by nickel (Ni) electroplating of SU-8 molds was reported [13]. Also, electroless plating was successfully applied for coating of silver on large microstructures opticaly fabricated in photo-curing resin [14]. The latter work emphasized the studies of metalization process of large polymeric structures, optically fabricated using a microlens array, as well as structural properties of the deposited silver film. Here we present a study in which optical fabrication of templates and their electrochemical metallization are aimed at producing MDPC structures exhibiting PBG behavior. In particular, we have fabricated dielectric templates with 3D woodpile architecture in SU-8 by DLW technique, performed their electroless coating by Ni film, and from analysis of their optical reflectivity spectra at infrared wavelengths have confirmed their PBG properties. The present study can be thus regarded as a step towards a simple and cost-effective practical fabrication of MDPC structures for IR spectral region.

2. Experimental techniques and details

The experimental procedure consists of three main stages. The first stage is fabrication of dielectric templates using DLW technique, the second stage is coating of the templates by Ni, and the last stage is assessment of their properties, which involved inspection by Scanning Electron Microscopy (SEM) and optical reflection measurements by micro Fourier-Transform Infrared (FTIR) spectroscopy. In addition to the experiments, theoretical modeling of photonic properties of the samples was conducted using a Finite-Difference Time-Domain (FDTD) technique. Below we will briefly describe these steps.

2.1. Preparation of dielectric templates

The templates were fabricated in a commercially available ultra-thick negative photoresist SU-8 NANO, formulation 50 from Microchem Corp. The processing of SU-8 followed the guidelines published in the manufacturer's web site. The photoresist was spin-coated to the thickness of about $30-50\,\mu$m on the cover glass substrates. Before and after the DLW the samples were soft-baked, and post-baked, respectively. After the DLW and post-bake, the samples were developed in a standard SU-8 developer and rinsed in isopropanol.

Principles of the DLW lithography are described in the existing literature [15, 16]; the DLW setup used in this study is almost identical to that employed in our earlier works [10, 12, 17, 18]. It used pulsed output of a Hurricane X system (Spectra-Physics) operatong at a repetition rate of 1 kHz, with pulse duration and central wavelength $\tau_{pulse} = 120\,$fs and $\lambda_{pulse} = 800\,$nm, cor-

#82675 - $15.00 USD Received 2 May 2007; revised 6 Jun 2007; accepted 8 Jun 2007; published 22 Jun 2007

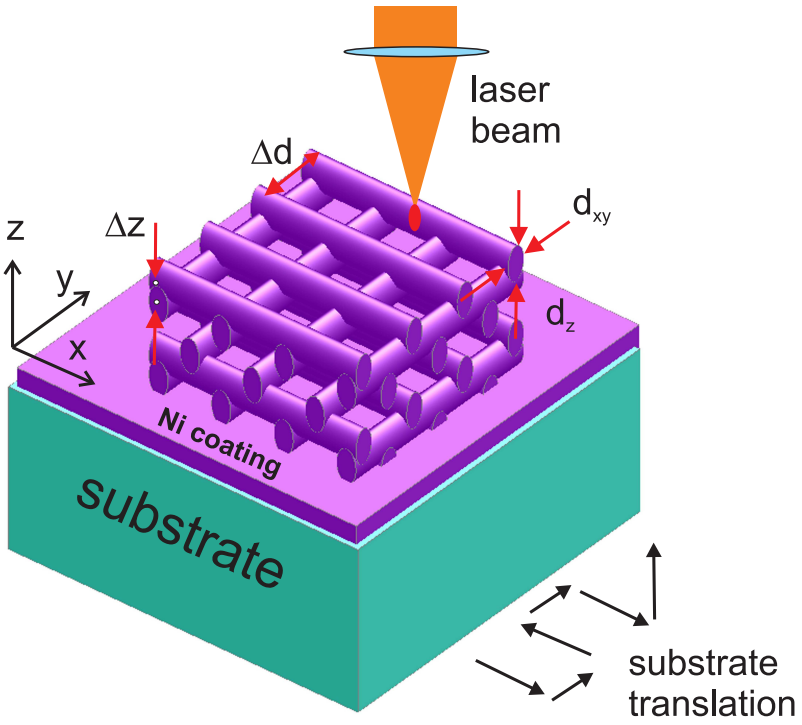

Fig. 1. 3D woodpile architecture and its main parameters. The scheme shows SU-8 woodpile structure fabricated on a glass substrate and coated by Ni. The main woodpile parameters are: Δd- distance between the centers of nearest two ellipsoidal rods on the same plane, Δz-vertical separation between the centers of rods belonging to two nearest planes, d_{xy} and d_z - minor and major axes of the ellipsoidal cross-section of the rod, m - total number of woodpile layers. Notice the $\Delta d/2$ parallel displacement between the rods in every second plane. Incidence of the focused laser beam and drawing of the woodpile by substrate translation during the DLW fabrication of SU-8 template are also illustrated schematically.

respondingly. The laser beam was coupled into Olympus IX71 optical microscope equipped with an objective lens (magnification 60×, numerical aperture NA=0.75). SU-8 is transparent at wavelengths $\lambda > 360-400$ nm, and therefore, two-photon absorption (TPA) or multi-photon absorption (MPA) are responsible for the absorption at λ_{pulse}, which occurs in a small spatial region located at the waist of the tightly focused beam. The absorption induces permanent photomodification of the photoresist by cross-linking of a polymer, which becomes stable against subsequent chemical development. The development removes unexposed SU-8, leaving only a solid exposed region. Drawing of 3D structures was accomplished by mounting the SU-8 coated substrate on a piezoelectric transducer-controlled 3D translation stage (a combination of P-517.2CL and P-518.ZCL stages from Physik Instrumente) with a positioning range of up to 100 μm and accuracy of several nanometers along each coordinate. The stage moved along a pre-defined path (see description below) during the exposure and linear features comprised of many overlapping exposed regions were recorded. Photoresist SU-8 is intended for optical fabrication of parts of micro-mechanical systems, therefore the recorded templates are mechanically and chemically stable.

3D woodpile architecture chosen for the recording was first suggested for DPC structures due

#82675 - $15.00 USD Received 2 May 2007; revised 6 Jun 2007; accepted 8 Jun 2007; published 22 Jun 2007

to its strong tendency to open a PBG at low index contrast, and the possibility of layer-by-layer assembly [19]. Since then, successful fabrication of woodpile structures by various techniques was reported in semiconductors [20, 21], metals [22], and in SU-8 [9, 11].

Figure 1 depicts schematically a Ni-coated woodpile consisting of layers of parallel rods, whose centers are separated by the distance Δd in the $x-y$ plane. The layers are stacked along the $z-$axis with layer-to-layer distance Δz. Mutual orientation of rods in the neighboring layers is perpendicular; rods in every other layer are displaced by half of the in-plane lattice period ($\Delta d/2$). During the DLW the woodpile is drawn in a rod-by-rod and layer-by-layer order, with the laser beam focused along the $z-$axis. Elongation of the focal region of the laser beam in the same direction results in rods having nearly elliptical cross-sectional shapes with minor and major axes d_{xy} and d_z, respectively. Estimation of the elongation factor d_z/d_{xy} will be described later. Parameters Δd and Δz are known almost exactly, since they are set by the motion of a high-accuracy 3D translation stage. Parameters d_{xy} and d_z depend non-linearly on the exposure conditions and therefore are more difficult to control. The choice of the woodpile structure parameters was aimed at obtaining mechanically stable samples whose PBG-related optical response would occur at IR wavelengths. The latter condition was verified by FDTD modeling (see below) prior to the fabrication.

2.2. Coating of SU-8 templates by Ni

Alkaline electroless Ni plating solution was chosen because of the low operating temperature ($30-40^{\circ}$C), which allows to minimize thermal effects in SU-8. It is also possible to use other electroless Ni plating solutions containing hypophosphite as a reducing agent. Although they would require higher temperatures of approximately $75-85^{\circ}$C [23], this is still somewhat lower than the thermal destruction threshold temperature of SU-8 ($>200^{\circ}$C in air [24, 25]).

The coating was carried out as follows. First, the samples were sensitized in the solution of $SnCl_2$ for 1 min, then washed in water, activated in solution of $PdCl_2$ for 1 min, and washed in water again. Afterwards, the samples were subjected to electroless plating of Ni in solution of $NiCl_2$, NH_4Cl, NaH_2PO_2, NH_4OH with pH = 9.2, at a temperature of $t = 40^{\circ}$C. Ni deposits obtained in such a procedure typically contain about 2 to 4% of phosphorus. Thickness of the Ni layer was controlled by the plating time. Thickness versus time dependence was calibrated by coating a copper plate under the same conditions as SU-8 structures, and measuring its mass increase. By setting the plating time from 4 to 7 min, thicknes could be adjusted in the range from 0.2 to 0.5 μm. For the woodpile samples, the duration was set to obtain coating thickness of 0.2-0.25 μm.

As far as the coating method is concerned, there are several differences between our work and another similar study dealing with metalization of optically fabricated structures by silver [14]. First, we have used Ni which requires both sensitization and activation, whereas for silver only the activation is required. Second, we have not attempted to prepare hydrophobic coating for the glass substrates. While skipping this step has allowed us to simplify preparation of the samples, it has also resulted in coating of the underlying substrate by Ni. The coated substrate therefore acts as a mirror located immediately behind the woodpile. Due to this reason our samples are not suited for optical characterization in transmission geometry along the $z-$axis direction. Nevertheless, they can still be characterized in the reflection geometry.

2.3. Studies of structural and optical properties

Visual inspection of the samples was performed using a scanning electron microscope (JSM-6700FT, JEOL). Infrared reflectivity spectra of the samples were measured in the spectral range of $1.8-12.0\,\mu$m using FT/IR-6000TM-M (Jasco) FTIR spectrometer equipped with an infrared microscope attachment. The microscope enables optical transmission and reflection measure-

#82675 - $15.00 USD Received 2 May 2007; revised 6 Jun 2007; accepted 8 Jun 2007; published 22 Jun 2007

ments of small samples with dimensions down to a few micrometers. In the microscope, radiation of a broadband IR source is focused on the sample and collected upon reflection by a Cassegrainian reflection objective with angular acceptance range of $\theta = 16 - 32^{\circ}$. During the measurements areas of the samples with size of about $(20 \times 20)\,\mu\text{m}^2$ were probed. The samples were oriented with woodpile stacking direction parallel to the optical axis of the focusing/collection optical system.

Numerical modeling of the structures' optical reflectivity was conducted using a commercial implementation of FDTD code, FDTD Solutions (Lumerical). The reflectivity was calculated by modeling propagation of a plane wave incident on the woodpile structure along the $z-$axis (layer stacking) direction and comparing the intensities of reflected and incident waves. The incident wave was a chirped pulse with a spectral width from 1.8 to $12.0\,\mu$m. The FDTD calculation region spanned one lattice period in the $x-y$ (layer) plane, with periodic boundary conditions. Along the $z-$axis (layer stacking) direction, perfectly-matched layer boundary conditions were imposed. The FDTD domain was discretized by a uniform cubic mesh with a period of 100 nm. The model woodpile parameters were assumed as close as possible to the real ones. Since thickness of the coated Ni layer was larger than the penetration depth of the optical radiation, optical properties of the underlying SU-8 templates were ignored, and the woodpiles were assumed to consist of monolithic Ni. Optical properties of Ni and their spectral dependencies were obtained from the literature [26].

3. Results and discussion

3.1. Structural properties

Figures 2 and 3 present SEM images of four structures as an illustration of the achievable quality and typical defects in the coated structures, all fabricated on the same glass substrate with mutual separation less than a few hundreds of micrometers. Hence, their coating by Ni was nearly identical The parameters of initial SU-8 templates are given in the figure captions. The main difference between the structures in Figs. 2 and 3 is smaller rod-to-rod and layer-to-layer distances in Fig. 3. In the next Section we will demonstrate that the structural downscaling leads to spectral scaling of photonic properties, which is a common feature of PBG materials.

Figures 2(a,b) illustrates that areas coated by Ni are predominantly smooth and grainless. At the same time, both images have darker, partially or fully "bare" areas. Detailed inspection of some of these areas, like the one shown in Fig. 2(b), reveals uncoated SU-8 and some Ni debris filling gaps between the rods. Such defects are unwanted as they will degrade optical quality of the samples. Another sample shown in Figs. 2(c,d), has fewer uncoated areas and a better overall quality. Its Ni-coated surface is smooth, with slight granularity apparent only near the boundaries of defective (uncoated) regions. These observations indicate polycrystalline character of the Ni film.

The difference in structural quality of samples fabricated on the same substrate can be explained by several factors. After the fabrication SU-8 templates were stored in ambient conditions for some time, and may have become unintentionally contaminated by dust, water or other environmental substances. Another possible factor is presence of gas bubbles during the deposition. Our preliminary studies have indicated that when the sensitization in $SnCl_2$ step was omitted, Ni coating was always rough and had rather patchy appearance. Contamination or gas bubbles may result in local areas insufficiently affected by SU-8 sensitization and activation. Preventing the contamination and applying additional cleaning, as well as using ultrasonic agitation during the deposition is expected reduce the undesired influences.

One can notice that the template of the sample with higher quality in Figs. 2(c,d) was fabricated at a lower laser pulse energy. This resulted in SU-8 rods of smaller diameter, and larger empty gaps separating the nearest surfaces of neighboring rods. Larger gaps may prevent ac-

#82675 - $15.00 USD Received 2 May 2007; revised 6 Jun 2007; accepted 8 Jun 2007; published 22 Jun 2007

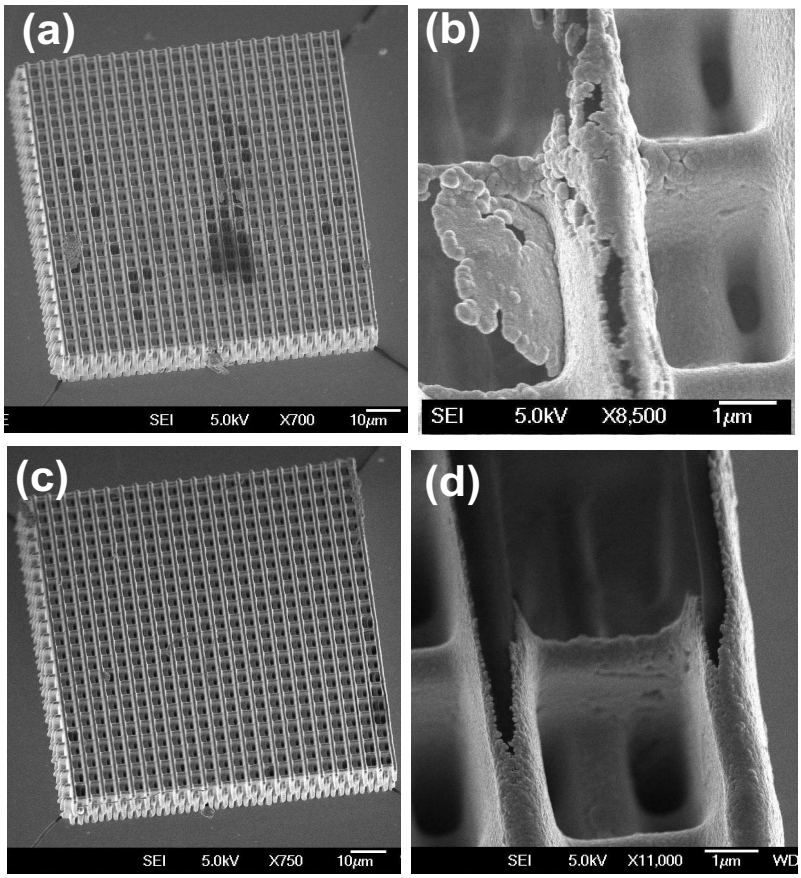

Fig. 2. SEM images of a SU-8 woodpile sample with lattice parameters $\Delta d = 4.0\,\mu$m, $\Delta z = 1.6\,\mu$m, size $(90 \times 90)\,\mu$m^2, thickness 10 layers, coated by a Ni layer with thickness of $0.3 \pm 0.05\,\mu$m, fabricated at a laser pulse energy of (a,b) 12 nJ (at the sample), (c,d) at a lower laser pulse energy of 8.5 nJ.

cumulation of Ni debris and speed up release of the gas bubbles, thus improving the overall structural quality.

Figure 3 shows images of two structures whose SU-8 templates have downscaled parameters, $\Delta d = 3.0\,\mu$m, and $\Delta z = 1.0\,\mu$m, compared to those in the previous Fig. Fabricated at similar laser pulse intensities, templates of these samples have lower air filling fraction due to more closely packed woodpile rods. Coating by Ni decreases the air fraction even further. One can notice signs of nearly-complete infiltration by Ni in Figs. 3(c,d). Therefore, in these areas only a few topmost woodpile layers will contribute to the optical reflectivity in a non-trivial manner.

3.2. Optical properties

Figures 4(a and b) show reflection spectra of the samples depicted in the previous Figs. For clarity, the spectra of samples having different woodpile parameters are displayed in different panels. All samples exhibit high reflectivity regions at long-wavelengths, with cut-off wavelengths for the samples with larger and smaller lattice parameters being approximately 6.0 and 4.4 μm, respectively. Maximum reflectivity of these regions vary from sample to sample, reaching about

#82675 - $15.00 USD Received 2 May 2007; revised 6 Jun 2007; accepted 8 Jun 2007; published 22 Jun 2007

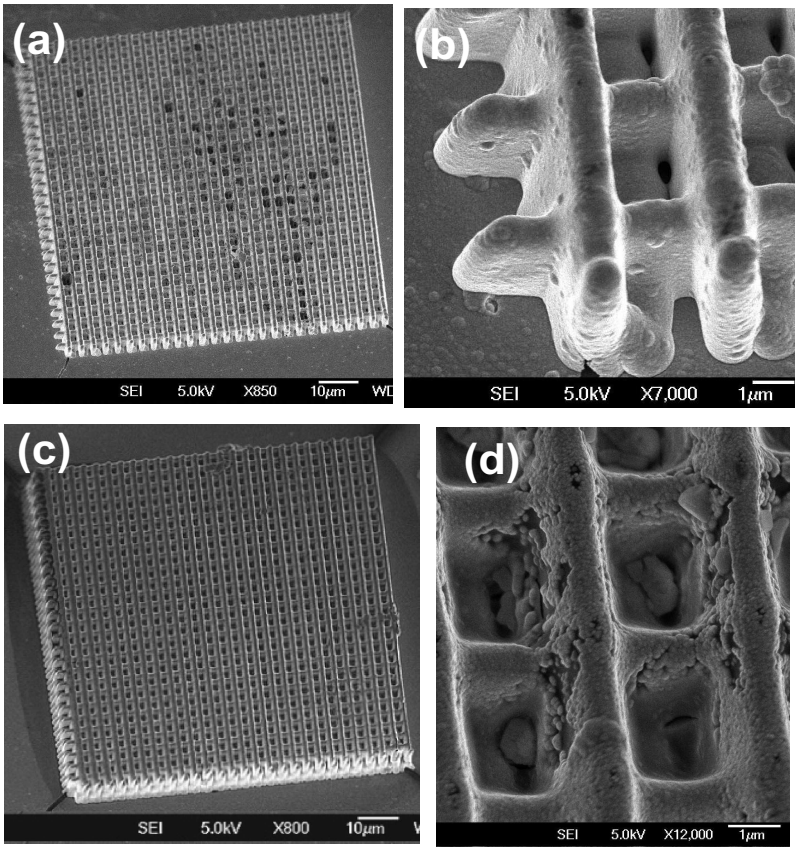

Fig. 3. SEM images of a SU-8 woodpile sample with slightly downscaled lattice parameters $\Delta d = 3.0\,\mu$m, $\Delta z = 1.0\,\mu$m, size, thickness and coating conditions identical to the sample shown in the previous Figure, fabricated at a laser pulse energy of (a,b) 8 nJ, (c,d) 10.0 nJ.

60% for the structure which has apparently highest structural quality (see Figs. 2(c,d)). The dependence of the cut-off wavelength on the period of the woodpile structure implies a strong role of photonic band dispersion. The long-wavelength high-reflectivity region is most likely a manifestation of so-called zero-order PBG, which is uniquely characteristic to MDPC systems. For 3D metallic wire-mesh structures the zero-order gap was demonstrated to extend to approximately half-frequency of the lowest-order conventional PBG [2].

All samples also exhibit weaker reflectivity peaks at shorter wavelengths. These peaks are most likely due to the first and higher-order PBG or stop-gaps (which are forbidden spectral regions for a single propagation direction). By comparing the spectra in both panels, one can see that reduction of lattice parameters leads to blue-shift of these reflectivity peaks. This Maxwell's scaling behavior is expected for PBG materials, and once again indicates that photonic band dispersion is the reason behind the observed reflectivity peaks.

We have verified these indications by comparing the experimental spectra with those obtained in numerical FDTD simulations. FDTD modeling depends on the choice of the structures' parameters. As mentioned earlier, the distances Δd and Δz are known with accuracy of a few nanometers. It is more difficult to find a suitable approximation for the cross-sectional shape of the rods. For bare SU-8 templates fabricated by DLW, the cross section is often assumed to

#82675 - $15.00 USD Received 2 May 2007; revised 6 Jun 2007; accepted 8 Jun 2007; published 22 Jun 2007

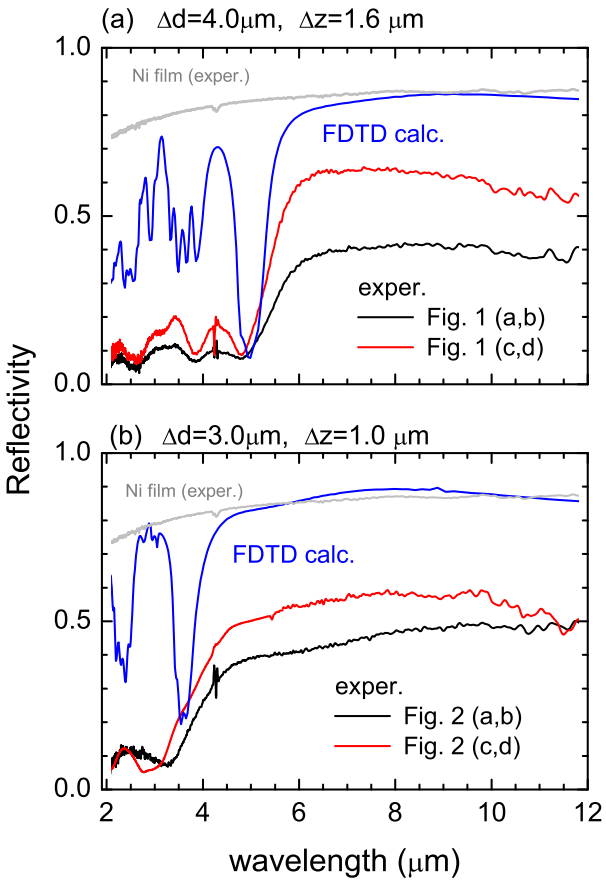

Fig. 4. Experimentally measured and numerically simulated reflection spectra of 3D woodpile structures coated by Ni.

be elliptical with elongation in the $z-$axis direction. We assume that the templates are coated by Ni film with uniform thickness; in this case the Ni-coated rods have elliptical cross-sections too. For the numerical aperture of the focusing objective NA=0.75, laser wavelength of $0.8\,\mu$m and diameter of the laser beam (before the focusing lens) of $d = 4.0\,$mm, elongation of the two-photon point-spread function (PSF) was estimated to be $d_z/d_{xy} \approx 4$. This evaluation was done numerically with the help of FDTD software. In all fabricated samples lateral diameter of SU-8 rods was $d_{xy} \approx 0.5-0.6\,\mu$m. After the coating by approximately $0.2-0.3\,\mu$m-thick layer of Ni, the diameters become $d_{xy} \approx 0.9-1.2\,\mu$m and $d_z \approx 2.4-3.0\,\mu$m. Lateral diameter of the coated rods can be easily determined from top-view inspection by SEM. We have found the actual value of $d_{xy} \approx 1.0\,\mu$m, in agreement with the above estimate. The longitudinal diameter $d_z \approx 2.0-2.4\,\mu$m can be estimated from the elongation ratio. Variation of the initial and estimated parameters is about 30%, which is sufficient for defining a model woodpile structure exhibiting optical properties qualitatively similar to those of the actual samples.

#82675 - $15.00 USD Received 2 May 2007; revised 6 Jun 2007; accepted 8 Jun 2007; published 22 Jun 2007

In FDTD calculations the probing wave is transmitted along the layer stacking ($z-$axis) direction. Thickness of the structure is assumed to comprise two lattice periods (eight woodpile layers) along this direction. To the rear side of the structure a monolithic block of Ni is attached in accordance to the experimental conditions. One can see that in these circumstances the reflected signal will consist of the wave reflected from the structure before reaching the substrate, expected to be a dominant contribution, and the wave that has reached the substrate, undergone multiple reflections between the structure and the substrate before escaping back. This wave is simultaneously affected by both reflection and transmission, and is expected to be a minor contribution to the reflected signal.

The simulated reflection spectra are included in each panel of Fig. 4 together with experimental data. As can be seen from the Fig., the calculated spectra reproduce essential features of the experimental ones. We would like to emphasize good matching between the spectral positions of various reflectivity features; difference in their strength can be explained by deviations between the idealized model and the actual samples and measurement conditions. Cut-off wavelengths of the zero-gap region, and reflectivity peaks corresponding to the higher-order photonic gaps are well reproduced by the calculations. However, the measured reflectivities are somewhat lower than the calculated ones. First of all, loss of reflectivity may occur due to dissipative losses in Ni (notice, that even FDTD calculations predict maximum reflectivity of about 85% in the zero-gap region, mostly due to the losses). This estimate agrees well with the experimental reflectivity of Ni film deposited on the glass substrate, which is also included in Figs. 4(a,b). Significant loss of reflectivity may also occur due to the Rayleigh scattering by random inhomogeneities. The Rayleigh scattering becomes progressively stronger at shorter wavelengths. Indeed, reflectivity peaks become weaker at shorter wavelength in the measured spectra. Moreover, Cassegrainian reflection objectives used in the infrared microscope of FTIR setup invariably probe and detect the reflection in a conical range of incidence angles (from 16 to 32° in our setup) around the normal to the sample's surface. Consequently, the measured reflectivities represent the result of angular and spectral averaging which typically leads to the loss of magnitude of spectral features. Finally the optically probed thickness of the actual structures may be different from the thickness used in FDTD modeling. As discussed above, in some areas of the samples air gaps between the rods may be filled by metallic Ni, or by random debri.

4. Conclusions

We have fabricated 3D metallic woodpile structures using a combination of DLW technique in photoresist SU-8 and electroless coating by Ni. Examination of structural and optical properties of the samples conducted in the course of this study allows to make favorable conclusions about the applicability of this method. The Ni-coated woodpile samples exhibit structural and optical quality, which can be informally rated as satisfactory. Fabrication of SU-8 templates by DLW is a relatively simple process, at least, compared to semiconductor microprocessing techniques, which in future can be used to obtain templates with other kinds of photonic architectures, and a higher resolution [11]. Also, holographic or interference recording technique can be used for fast fabrication of large SU-8 templates [27, 28] suitable for metallization. Electroless coating is a low-cost and fast process which allows coating of complex surfaces by smooth metallic films with controllable thickness. Although Ni, which is somewhat more lossy than noble metals Au or Ar, is not the most desired material for MDPC structures, deposition of other metals such as Co, Cu, Pd, Ag and Au using the same approach is possible [29, 30]. For electroless Co and Pd plating, hypophosphite plays the role of reducing agent, whereas for Cu-plating formaldehyde is used [31]. Electroless deposition of Cu, Ag and Au using cobalt(II) complexes has also been studied [32]. Moreover, Ni-coated structures can be further infiltrated by gold, silver, or other low-loss metals using simple chemical (as opposed to electrochemical) methods.

#82675 - $15.00 USD Received 2 May 2007; revised 6 Jun 2007; accepted 8 Jun 2007; published 22 Jun 2007

Thus, the combination of DLW and electroless coating provides a versatile tool for the creation of MDPC structures for IR spectral range. It is expected that this study will be helpful for the development of fabrication methods of metalo-dielectric photonic and optoelectronic systems.

#82675 - $15.00 USD Received 2 May 2007; revised 6 Jun 2007; accepted 8 Jun 2007; published 22 Jun 2007